International Journal of Mechanical, Industrial and Aerospace Sciences
ISSN: 2517-9950
Vol:5, No:1, 2011

CFD Simulation of Non-Newtonian Fluid Flow in Arterial Stenoses with Surface Irregularities

R. Manimaran

***Abstract*—**CFD simulations are carried out in arterial stenoses with 48 % areal occlusion. Non-newtonian fluid model is selected for the blood flow as the same problem has been solved before with Newtonian fluid model. Studies on flow resistance with the presence of surface irregularities are carried out. Investigations are also performed on the pressure drop at various Reynolds numbers. The present study revealed that the pressure drop across a stenosed artery is practically unaffected by surface irregularities at low Reynolds numbers, while flow features are observed and discussed at higher Reynolds numbers.

***Keywords*—**Blood flow, Roughness, Computational fluid dynamics, Bio fluid mechanics.

I. Introduction

THE flow situation in stenosis models has previously been studied for different Reynolds number and different constrictions of the cross-sectional area. The steady state problem is easier to solve numerically and yet adequately describes the happening of flow and pressure around constrictions of blood vessels in the arterial pipes [1]. Measurement of velocity profiles in blood vessels has been carried out by means of pulsed ultrasound Doppler flowmeters. However, the space resolution of this instrument is poor, especially along the wall. CFD studies are also performed using commercial packages in obtaining the knowledge on flowfield [2].

Experimental investigations which have been carried out on physical models have mainly been concerned with measuring flow velocities by LASER Doppler flow meter, visualization of streamlines either by contrast dye or hydrogen bubbles [3]. The large amount of data which has to be collected in order to map velocity profiles by the digital instruments especially for non-newtonian flow has never been attempted before [4].

The idea behind this paper is to compare the effects of different non-newtonian models on the wall shear stress distributions in the right coronary artery. The studies in the coronary artery during the cardiac cycle have already been carried out [5], [6]. The comparison among non-newtonian models such as Herschel-Bulkley, Carreau model and power law will allow us to assess whether or not it is necessary to include non-Newtonian blood models in modelling blood flow in coronary arteries [7].The flow of blood within arteries has long been associated with the formation of lesions and, eventually, arterial narrowing. Experimental and numerical investigation of these relationships has been the subject of recent reviews [8],[9] & [10]. Much of the early numerical modelling was focused on the carotid artery bifurcation ([11],[12],[13],[14 [15],[16]), but, recently, this focus has shifted to the right coronary artery, both in terms of simulation [17],[18],[19] & [20]. It is well known that blood is a non-Newtonian fluid [21] and several models have been proposed to predict the stress–strain relationship for blood [22]. However, some of these models is generally accepted as a reflection of the true behaviour of the rheology of blood. This is, perhaps, the reason that blood should be chosen as a non-newtonian fluid rather than a Newtonian fluid in simulations of blood flow. It is also generally accepted that blood behaves as a non-Newtonian fluid at shear rates above 100 s^{-1} [23] which may account for the Newtonian approximation in flow simulations at larger Reynolds numbers. However, studies in bifurcations and long arteries, especially when the flow stops, there are periods of time where the shear rate is above 100 s^{-1} [24] and non-Newtonian effects could become important. There does not appear to be a consensus in the literature on the importance of non-Newtonian effects on steady flows in large arteries. Some studies found non-Newtonian theology as important [25],[26] and [27], while others found that it is relatively unimportant [28],[29][30] in determining flow patterns in large arteries. The research paper by [31] contains a good discussion of possible reasons for this discrepancy, particularly in the light of their definition of the non-Newtonian importance factor. A more recent comparison has been conducted for flow through a curved tube [32], which highlights several differences between Newtonian and non-Newtonian flow patterns. The paper also describes the calculation of an effective Newtonian viscosity which captures the non-Newtonian effects for this flow situation. Comparisons between the various arteries and blood viscosity models are presented in terms of wall shear stress distributions as it is believed that wall shear stress is a significant factor in the onset of coronary artery disease [33],[34]&[35]. Further comparisons are presented in terms of the recently generalized [36] local and global non-Newtonian importance factors [37]. It is worth noting that the various non-Newtonian blood models are obtained by parameter fitting to experimental viscosity data obtained at certain shear rates under steady-state conditions [38]. Here, it is assumed that these models can be used under steady as well as pulsatile flow conditions. The work here, however, involves a comparison of wall shear stress distributions, which are obtained using both the Newtonian and non- Newtonian models of blood viscosity.

R. Manimaran is with the School of Mechanical and Building Sciences, Vellore Institute of Technology University, Vellore, Tamilnadu India 632014 (phone: +91416-2202268 e-mail: manimaran.r@vit.ac.in).

So, while major differences between the results of these two models would need to be examined in the light of the above comments, similar results for the models would indicate that this assumption is most likely a reasonable one.

II. Background

The model for blood flow through a mild arterial stenosis originates from an in-vitro investigation of flow in a mildly atherosclerotic main coronary artery casting of man conducted by Back et al. (1984) [1]. Since the local cross sections were generally noncircular and the orientation of the axis of the cast varied along the vessel, experiments were also carried out in an analogous straight and axisymmetric model having the same cross-sectional area variation as the actual cast [3]. In the present study, we follow Johnston and Kilpatrick [6] and restrict the computational flow analysis to the axisymmetric stenosis model.

III Mathematical Modelling

It will be assumed that the flow of blood in the right coronary artery is governed by the Navier–Stokes equations.

$$\rho(\frac{\partial V}{\partial t} + V.\nabla V) = -\nabla.\tau - \nabla P \quad (1)$$

and the continuity equation for an incompressible fluid.

$$\nabla.V = 0 \quad (2)$$

In these equations, V is the two-dimensional velocity vector, t the time, P the pressure, ρ the density and τ the stress tensor. Writing the Navier–Stokes equations in this form allows the flexibility to use an arbitrary non-Newtonian blood model. However further in the experiments, Back et al. (1984)[1] used sugar water solutions as test fluids to simulate the viscosity of blood. Here, we simply follow Johnston and Kilpatrick (1991) [6] and assume that the fluid is incompressible and non-Newtonian. The steady flow through the stenosed artery model is therefore governed by the stationary conservation equations for mass and momentum, i.e. the Navier Stokes equations. The equations were solved using the commercially available software package Ansys FLUENT 6.3 [2] for performing computational fluid dynamics simulations. The implications besides the substantial guiding impact of the stenosis wall, along which conventional no-slip boundary conditions are imposed, the mathematically formulated flow problem is controlled solely by the Reynolds number

$$\mathrm{Re} = \frac{\rho V D}{\mu} \quad (3)$$

Where ρ and μ are the density and the dynamic viscosity of the fluid considered.

IV. Geometrical Model

The three geometrically different models of the stenosis shape shown in Fig. 1 have been examined, all with 48% areal occlusion and thus classified as mild. The first shape considered is the most commonly used cosine curve

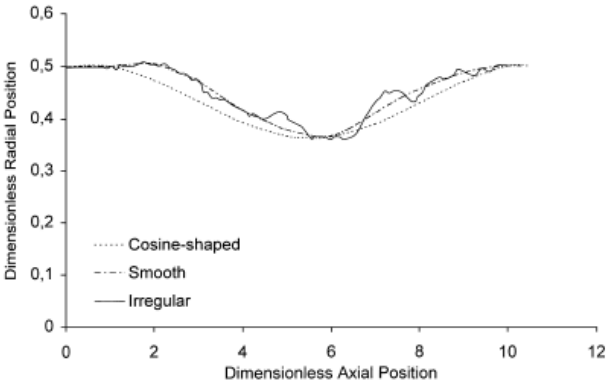

Fig. 1 Comparison of the three different stenosis models considered. Dimensionless radial position $R(z)/D$ versus dimensionless axial position

Radius R is given as function of Z the axial length

$$R(Z) = 0.5D - 0.5\delta * (1 + \cos(\pi(2Z - L))/L) \quad (4)$$
$$for\ 0 \le Z \le L$$

originally suggested by Young (1968) where L is the length and δ is the maximum width of the stenosis. Thus, with $\delta = 0.138D$, the area occlusion $1 - (1 - 2\delta / D)^2$ becomes 0.48. The second geometrical model considered is the straight axisymmetric model of Back et al. (1984) [1], which mimics real surface irregularities since the actual axial variation of the cross-sectional area of a left circumflex coronary artery casting from a human cadaver is retained. The profile of this irregular stenosis model has been provided both by Back et al. (1984) [1] and Johnston and Kilpatrick (1991) [6]. Finally, a smooth stenosis model will be studied. This new model exhibits the same general form as the irregular stenosis model, but surface irregularities or roughness elements are absent. This stenosis model can therefore be considered as smooth, but in contrast to the cosine-shaped model, the profile of this stenosis is no longer symmetric about its centre (i.e. the narrowest point). The profiles of the cosine-shaped, the irregular and the smooth stenoses are compared in Fig. 1.

V. Viscosity Models

The mathematical model, i.e. the Navier Stokes equations, is solved numerically by means of a finite volume method using the commercially available Ansys FLUENT package. The element mesh for each geometrical configuration is constructed with the GAMBIT (Fluent Inc.). SIMPLE algorithm is employed for solving the Navier-Stokes equations for incompressible fluid. The solution is marched towards steady state and residuals are monitored until it reaches the convergence criterion of 10^{-6}. Grid independent studies are performed and found that the interior domain of 2 lakh cells provide a smooth solution and higher number of cells resulted in same situation as found with 2 lakh cells. The main consideration in this paper is about the usage of non- Newtonian fluid models and they are briefly described below.

Herschel Bulkley Model

$$\frac{\partial p}{\partial x} = \frac{\partial}{\partial z}\left(\mu \frac{\partial u}{\partial z}\right) = \begin{cases} \mu_0 \frac{\partial^2 u}{\partial z^2}, & \left|\frac{\partial u}{\partial z}\right| < \gamma_0 \\ \frac{\partial}{\partial z}\left[\left(k\left|\frac{\partial u}{\partial z}\right|^{n-1} + \tau_0 \left|\frac{\partial u}{\partial z}\right|^{-1}\right)\frac{\partial u}{\partial z}\right], & \left|\frac{\partial u}{\partial z}\right| \geq \gamma_0 \end{cases}$$

where Π is the second invariant of the rate-of-strain tensor:

$$\Pi = \sqrt{2E_{ij}E^{ij}}$$

If n=1 and $\tau_0 = 0$, this model reduces to the Newtonian fluid. If n<1 the fluid is shear-thinning, while n>1 produces a shear-thickening fluid. The limiting viscosity μ_0 is chosen such that $\mu_0 = k\Pi_0^{n-1} + \tau_0\Pi_0^{-1}$. A large limiting viscosity means that the fluid will only flow in response to a large applied force. This feature captures the Bingham-type behaviour of the fluid.

Carreau Model : In this type, a generalized Newtonian fluid where viscosity, μ_{eff}, depends upon the shear rate, $\dot{\gamma}$, by this equation: $\mu_{\text{eff}}(\dot{\gamma}) = \mu_0\left(1 + (\lambda\dot{\gamma})^2\right)^{\frac{n-1}{2}}$ Where: μ_0, λ and n are material coefficients. At low shear rate ($\dot{\gamma} \ll 1/\lambda$) Carreau fluid behaves as a Newtonian fluid and at high shear rate ($\dot{\gamma} \gg 1/\lambda$) as a power-law fluid.

Non-Newtonian power law : A Power-law fluid, or the Ostwald–de Waele relationship, is a type of generalized Newtonian fluid for which the shear stress, τ, is given by velocity gradient of power 'n' with μ is the flow consistency index (SI units Pa•s^n), $\partial u/\partial y$ is the shear rate or the velocity gradient perpendicular to the plane of shear (SI unit s^{-1}), and n is the flow behaviour index (dimensionless). The quantity $\mu_{\text{eff}} = K\left(\frac{\partial u}{\partial y}\right)^{n-1}$ represents an apparent or effective viscosity as a function of the shear rate (SI unit Pa•s).

VI. Results and Discussion

Three cases are considered here for various Reynolds numbers. The non-dimensional pressure drop is calculated for different Reynolds number as shown in Fig.2 for three different viscosity models considered. The Carreau model predicts the flow compared to data provided by the experiments [1]. However, other models did follow the trend but still lack in accuracy.

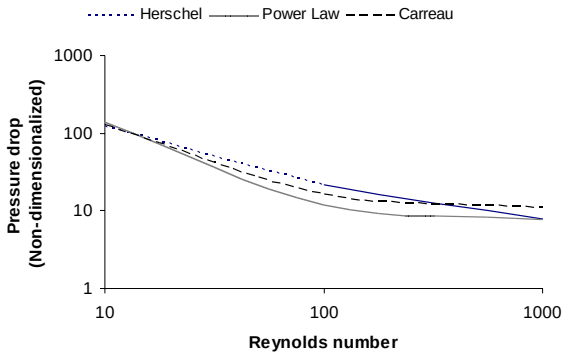

Fig. 2 Non-dimensional drop versus Reynolds number for different viscosity models

The non-dimensional pressure drop is plotted in Fig. 3 for different geometries considered before. The cosine shaped profile predicts the flow better as compared to smooth and irregular geometries at higher Reynolds numbers.

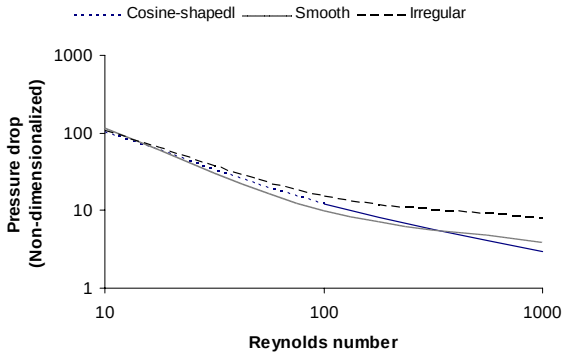

Fig. 3 Non-dimensional drop versus Reynolds number for different geometries

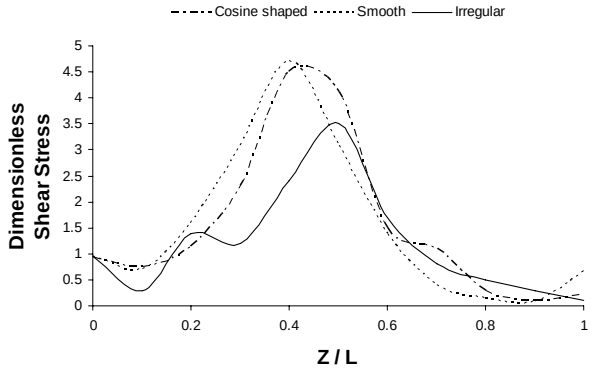

Fig. 4 Dimensionless wall shear stress versus non-dimensional

axial length at Re = 10 for different geometries

The shear stress varies correspondingly for different geometries chosen and plotted in Fig. 4. The cosine profile shows the highest stress among the geometries considered at Re=10. The irregular geometry shows higher stress at higher Reynolds number (Re=1000) in the Fig. 5. This is because of the flow is getting affected due to surface irregularities as shear stress is directly proportional to friction factor in a pipe flow (Hagen Poiseuille formula). Figures 4 and 5 are plotted for Carreau model and different geometries. The dimensionless center line velocity is calculated and plotted in figures 6 and 7 for Newtonian and Carreau models at Re = 10 and 1000. It can be seen that Carreau model slightly peaks at the middle length of stenoses and considered to be prominent.

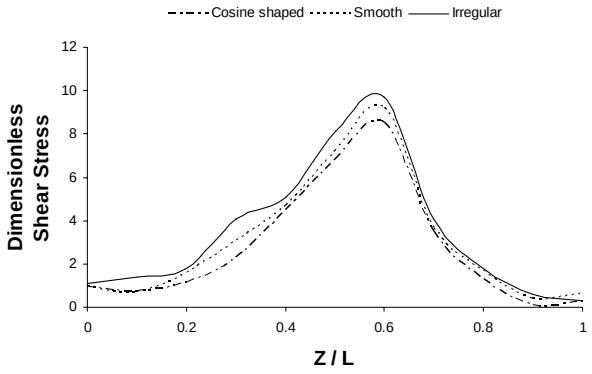

Fig. 5 Dimensionless wall shear stress versus non-dimensional axial length at Re = 1000 for different geometries

The contours for cosine shaped profile following Carreau model are shown in figures 8, 9, 10, 11 and 12. The deformation of fluid become maximum at the throat of the stenoses as seen in Fig. 8. The radial velocity gradients (dv/dx) are negligible and can be ignored compared to dv/dy. The axial velocity gradients are found to be higher near the axis at the middle of stenoses and lower near the wall. The radial velocity in Fig. 12 is shown contrary of Fig. 9 so that

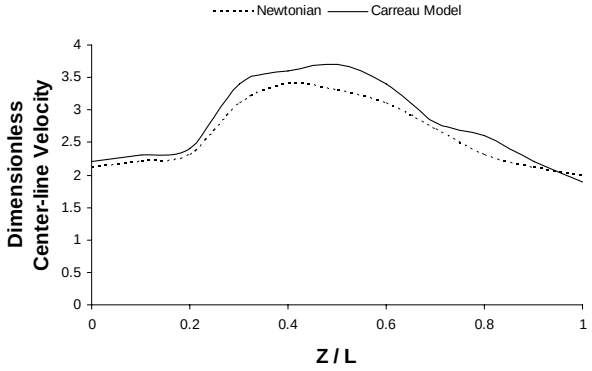

Fig. 6 Dimensionless center-line velocities versus non dimensional axial length at Re = 10

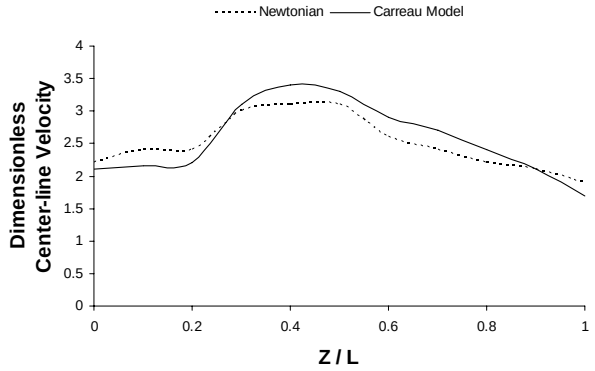

Fig. 7 Dimensionless center-line velocities versus non-dimensional axial length at Re = 1000

the summation of quantities du/dx and dv/dy should be equal to zero according to continuity equation. The dimensionless vorticity contours represent the spin rate of fluid particles in the domain. Because of the nature of rotational flow at the throat, the circulation of blood in this region is enhanced. The diverging part contains a little recirculation region as evident in Fig. 14. This is due to the larger divergence angle and flow leads to turbulent regime. The suitability of a turbulence in predicting the flow at this zone may throw light in further research and reduce the lacunae. The simulation performed in this case presents a situation where flow can be reasonably predicted with Carreau model appropriate to the experimental data discussed in the review [10].

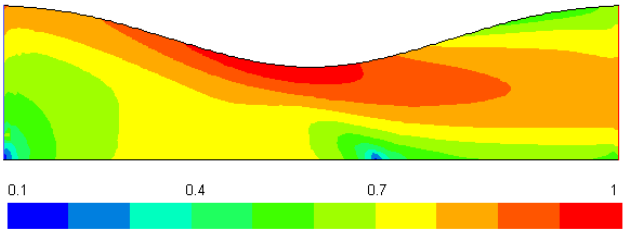

Fig. 8 Dimensionless shear strain rate (du/dy+dv/dx) contours at Re = 1000 for a Cosine geometry and Carreau model

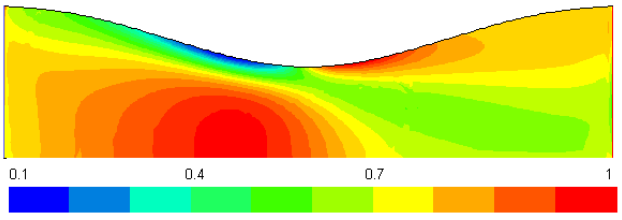

Fig. 9 Dimensionless axial velocity gradient contours (du/dx) at Re = 1000 for a Cosine geometry and Carreau model

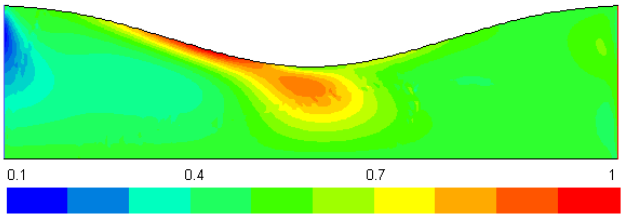

Fig. 10 Dimensionless radial velocity gradient (dv/dx) contours at Re = 1000 for a Cosine geometry and Carreau model

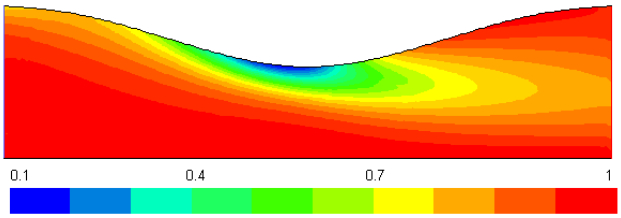

Fig. 11 Dimensionless axial velocity gradient (du/dy) contours at Re = 1000 for a Cosine geometry and Carreau model

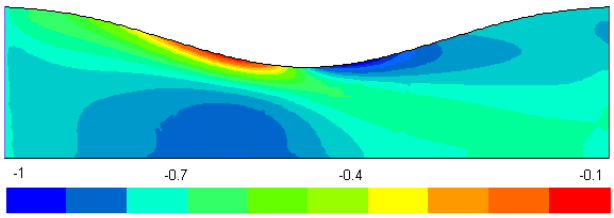

Fig. 12 Dimensionless axial velocity gradient (dv/dy) contours at Re = 1000 for a Cosine geometry and Carreau model

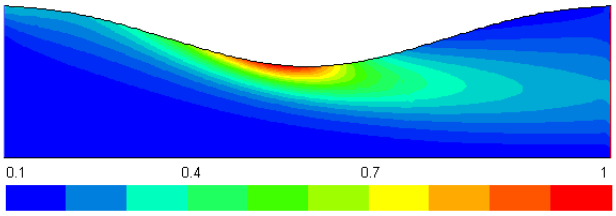

Fig. 13Dimensionless vorticity contours (dv/dx - du/dy) at Re = 1000 for a Cosine geometry and Carreau model

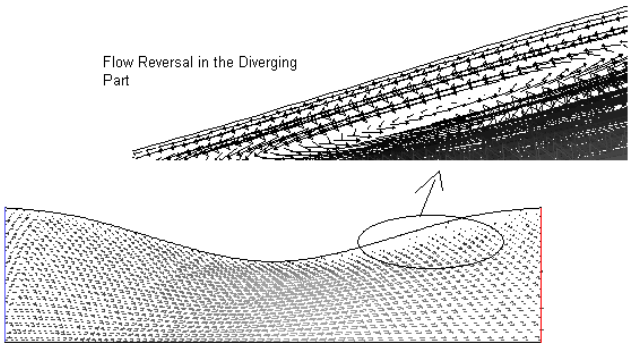

Fig. 14 Recirculation zone in the diverging part at Re = 1000 for a Cosine geometry and Carreau model

VII. Conclusion

It is observed from this study that the rheological properties of blood can significantly affect the flow phenomena. For the steady state case, the results indicate that the non-Newtonian effects weaken the distortion of flow pattern, pressure distribution and wall shear stress associated with the areal occlusion of 48 % in arterial stenosis. As Reynolds number increases, the pressure drop decreases independent of non-newtonian models, whereas in Carreau model predicts closer to the experimental results. Further, the contours of wall shear stress is prominent between two different Reynolds numbers for the Carreau model selected, which predicts the experimental data. A small recirculation region is found which may affect the flow in coronoid artery.

Carreau model gives rise to stronger vorticity production at the throat, and the streamlines and velocity profiles indicate that the flow patterns remain in a disturbed state over a long distance. The pressure drop and the wall shear stress are smaller for the Newtonian cases, as in the steady flow. The results demonstrate that the Carreau model is capable of predicting the haemodynamic features most interesting to physiologists. It can be used to predict fast stenotic flow patterns on an individual basis. It can also be used for studying other parametric effects.

References

[1] Back, L.H., Cho, Y.I., Crawford, D.W., Cuffel, R.F., 1984. Effect of mild atherosclerosis on flow resistance in a coronary artery casting of man. ASME Journal of Biomechanical Engineering 106, 48-53.
[2] Fluent Inc., 2006. Fluent User's Guide.
[3] Haldar, K., 1985. Effects of the shape of stenosis on the resistance to blood flow through an artery. Bulletin of Mathematical Biology 47, 545-550.
[4] Hellevik, L.R., Kiserud, T., Irgens, F., Ytrehus, T., Eik-Nes, S.H., 1998.
[5] Simulation of pressure drop and energy dissipation for blood flowin a human fetal bifurcation. ASME Journal of Biomechanical Engineering 120, 455-462.
[6] Johnston, P.R., Kilpatrick, D., 1991. Mathematical modelling of flow through an irregular arterial stenosis. Journal of Biomechanics 24, 1069-1077.
[7] Young, D.F., 1968. Effect of a time dependent stenosis on flow through a tube. ASME Journal of Engineering for Industry 90, 248-254.
[8] Asakura, T., Karino, T., 1990. Flow patterns and spatial distribution of atherosclerotic lesions in human coronary arteries. Circulation Research 66, 1054–1066.
[9] Ballyk, P.D., Steinman, D.A., Ethier, C.R., 1994. Simulation of non-Newtonian blood flow in an end-to-end anastomosis. Biorheology 31 (5), 565–586.
[10] Berger, S.A., Jou, L.-D., 2000. Flows in stenotic vessels. Annual Review of Fluid Mechanics 32, 347–382.
[11] Berthier, B., Bouzerar, R., Legallais, C., 2002. Blood flow patterns in an anatomically realistic coronary vessel: influence of three different reconstruction methods. Journal of Biomechanics 35, 1347–1356.
[12] Caro, C.G., 2001. Vascular fluid dynamics and vascular biology and disease. Mathematical Methods in the Applied Sciences 24, 1311–1324.
[13] Caro, C.G., Fitz-Gerald, J.M., Schroter, R.C., 1971. Atheroma and arterial wall shear: observation, correlation and proposal of a shear dependent mass transfer mechanism for atherogenesis. Proceedings of the Royal Society of London B 177, 109–159.
[14] Cho, Y.I., Kensey, K.R., 1991. Effects of the non-Newtonian viscosity of blood on flows in a diseased arterial vessel. Part 1: steady flows. Biorheology 28, 241–262.

[15] Corney, S., Johnston, P.R., Kilpatrick, D., 2001. Cyclic flow patterns in human coronary arteries. In: Computers in Cardiology, IEEE Press, New York, pp. 21–24.
[16] Corney, S., Johnston, P.R., Kilpatrick, D., 2004. Construction of realistic branched, three-dimensional arteries suitable for computational modelling of flow. Medical and Biological Engineering and Computing 42, 660–668.
[17] Feldman, C.L., Ilegbusi, O.J., Hu, Z., Nesto, R., Waxman, S., Stone, P.H., 2002. Determination of in vivo velocity and endothelial shear stress patterns with phasic flow in human coronary arteries: a methodology to predict progression of coronary atherosclerosis. American Heart Journal 143, 931–939.
[18] Fry, D., 1968. Acute vascular endothelial changes associated with increased blood velocity gradients. Circulation Research 22, 165–197.
[19] Fung, Y.C., 1993. Biomechanics: Mechanical Properties of Living Tissues, second ed. Springer, Berlin.
[20] Giddens, D.P., Zarins, C.K., Glagov, S., 1990. Response of arteries to near wall fluid dynamic behavior. Applied Mechanics Review 43 (2), S98–S102.
[21] Gijsen, F.J.H., Allanic, E., van de Vosse, F.N., Janssen, J.D., 1999. The influence of the non-Newtonian properties of blood on the flow in large arteries: unsteady flow in a curved tube. Journal of Biomechanics 32, 705–713.
[22] Johnston, B.M., Johnston, P.R., Corney, S., Kilpatrick, D., 2004. Non-Newtonian blood flow in human right coronary arteries: steady state simulations. Journal of Biomechanics 37 (5), 709–720.
[23] Kirpalani, A., Park, H., Butany, J., Johnston, K.W., Ojha, M., 1999. Velocity and wall shear stress patterns in the human right coronary artery. Journal of Biomechanical Engineering 121, 370–375.
[24] Krams, R., Wentzel, J.J., Oomen, J.A.F., Vinke, R.H., Schuurbiers, J.C., de Feyter, P.J., Serruys, P.W., Slager, C.J., 1997. Evaluation of endothelial shear stress and 3D geometry as factors determining the development of atherosclerosis and remodelling in human coronary arteries in vivo—combining 3D reconstruction from angiography and IVUS (ANGUS) with computational fluid dynamics. Arteriosclerosis, Thrombosis and Vascular Biology 17, 2061–2065.
[25] Ku, D., Giddens, D., Zarins, C., Glagov, S., 1985. Pulsatile flow and atherosclerosis in the human carotid bifurcation: positive correlation between plaque and low and oscillating shear stress. Arteriosclerosis 5, 293–302.
[26] Liepsch, D., 2002. An introduction to biofluid mechanics—basic models and applications. Journal of Biomechanics 35, 415–435.
[27] Matsuo, S., Tsuruta, M., Hayano, M., Immamura, Y., Eguchi, Y., Tokushima, T., Tsuji, S., 1988. Phasic coronary artery flow velocity determined by Doppler flowmeter catheter in aortic stenosis and aortic regurgitation. The American Journal of Cardiology 62 (1), 917–922.
[28] Myers, J.G., Moore, J.A., Ojha, M., Johnston, K.W., Ethier, C.R., 2001. Factors influencing blood flow patterns in the human right coronary artery. Annals of Biomedical Engineering 29,109–120.
[29] Ojha, M., Leask, R.L., Butany, J., Johnston, K.W., 2001. Distribution of intimal and medial thickening in the human right coronary artery: a study of 17 RCAs. Atherosclerosis 158, 147–153.
[30] Pedley, T.J., 1980. The Fluid Mechanics of Large Blood Vessels. Cambridge University Press, Cambridge.
[31] Perktold, K., Resch, M., 1990. Numerical flow studies in human carotid artery bifurcations: basic discussion of the geometry factor in atherogenesis. Journal of Biomedical Engineering 12, 111–123. Perktold, 409–420.
[32] Rodkiewicz, C.M., Sinha, P., Kennedy, J.S., 1990. On the application of a constitutive equation for whole human blood. Journal of Biomechanical Engineering 112, 198–206.
[33] Tu, C., Deville, M., 1996. Pulsatile flow of non-Newtonian fluids through arterial stenoses. Journal of Biomechanics 29 (7), 899–908.
[34] van de Vosse, F.N., Gijsen, F.J.H., Wolters, B.J.B.M., 2001. Numerical analysis of coronary artery flow. In: 2001 Bioengineering Conference, vol. 50. ASME, New York, pp. 17–18.
[35] van Langenhove, G., Wentzel, J.J., Krams, R., Slager, C.J., Hamburger, J.N., Serruys, P.W., 2000. Helical velocity patterns in a human coronary artery. Circulation 102, e22–e24.
[36] Walburn, F.J., Schneck, D.J., 1976. A constitutive equation for whole human blood. Biorheology 13, 201–210.
[37] Wentzel, J.J., Gijsen, F.J.H., Stergiopulos, N., Seruys, P.W., Slager, C.J., Krams, R., 2003. Shear stress, vascular remodeling and neointimal formation. Journal of Biomechanics 36, 681–688.
[38] Zeng, D., Ding, Z., Friedman, M.H., Ethier, C.R., 2003. Effects of cardiac motion on right coronary artery hemodynamics. Annals of Biomedical Engineering 31, 420–429.
[39] Zhu, H., Warner, J.J., Gehrig, T.R., Friedman, M.H., 2003.Comparison of coronary artery dynamics pre- and post-stenting. Journal of Biomechanics 36, 689–697.